

Research Article

Variation of Compton Profiles of N₂ with Increasing Pressures

*Erdem Sakar^a, Ali Gürol^{*a}, Osman Yücel^b*

^aAtatürk University, Faculty of Science, Phys, Dept., 25240, Erzurum, Türkiye

^bAtatürk University, Vocational School of Health Services, 25240, Erzurum, Türkiye

Abstract

In this study, it has been measured the Compton Profile of the Nitrogen gas at different pressures by using a Compton Profile Spectrometer with an annular Am-241 radioactive source, which emits 59.537 keV photons. The inelastic scattered γ -rays from gas molecules in a gas chamber have been measured using a HPGe detector connected to the a Tennelec 244 Amplifier and MAESTRO MCA Software. The gas pressure had been set by using a manometer before the measurements. The data have been corrected for all environmental scattering effects, i.e. scattering from gas chamber's walls, collimators, and etc. Then, the Compton Profile of Nitrogen gases at five different pressures have been determined using a Matlab Code. We found that the Compton Profiles changes with increasing pressures.

Keywords: Compton Profile, Pressure, Nitrogen gas, Electron Momentum Distribution.

Artan Basınç ile N₂'nin Compton Profilelerinin Değişimi

Öz

Bu çalışmada, 59.537 keV enerjili γ -ışınları yayınlayan bir Am-241 radyoaktif kaynağa sahip Compton Spektrometresi kullanılarak azot gazının Compton Profilleri ölçüldü. Bir gaz odasına hapsedilmiş gaz moleküllerinden inelastic olarak saçılmış γ -ışınları Tennelec 244 Yükseltici ve MAESTRO MCA Programına bağlanmış bir HPGe dedektör kullanılarak ölçüldü. Ölçümlerden önce gaz basıncı bir manometre ile ayarlandı. Bütün çevresel saçılma etkileri (gaz odasının duvarlarından, kolimatörlerden, vs., saçılmalar gibi) için ham veriler düzeltildi. Daha sonra, beş farklı basınçta azot gazının Compton Profileri Matlab'de yazılmış bir program ile belirlendi. Compton Profile değerlerinin artan basınçla değiştiği belirlendi.

Anahtar Kelimeler: Compton Profile, Basınç, Azot gazı, Elektron Momentum Dağılımı.

* Corresponding author
e-mail: agurol@atauni.edu.tr

Received: 17.10.2016
Accepted: 11.11.2016

Introduction

The inelastic scattering of a γ -ray photon from a charged particle, usually an electron in a target, with a large energy and momentum transfer, is referred to as Compton scattering. The inevitable quantum mechanical motion of the target electrons leads to a Doppler shift of the Compton scattered photon and thereby to a broadening of the Compton lineshape. This so-called Compton Profile (CP) furnishes important information about the momentum distribution of the target electrons. The interpretation of this broadening can be explained by Impulse Approximation (IA) (1). The IA assumes that the electrons that are doing the scattering may be treated as free rather than bound (2). During the scattering, the other electrons are in the same potentials. The momentum of the target electron is strongly related to the line broadening of the Compton peak. This leads to calculate the electron momentum density of target atoms. Thus, CP technique has been used for a large number of aims.

CP method has some characteristics, which other methods do not have for measuring the electron momentum distribution. Firstly, it gives not only momentum states of outer shell electrons which are of concern in quantum chemistry and solid state physics but also momentum states of inner shell electrons which are of concern in atomic and radiation physics. Secondly, since the scattering of each electron is independent of the scattering of others. Therefore, an impure target is the same as that from a pure crystal sample. This majorly simplified the preparation of samples. Lastly, CP method provides many qualitative conclusions about some properties of electrons in molecule and solids. Due to these characteristics, the CP method has been widely used in recent years in different areas of physics (3).

In the literature, many experimental and theoretical studies have been carried out

to determine the CPs for different elements and molecules. Theoretical studies were based on various calculation methods; such as Hartree-Fock (HF) and Density Functional Theory (DFT). Biggs et al. (4) calculated the CP for all the orbitals of all free atoms up to $Z=104$ by using HF method. Huotari et al. (5) and Holzman et al. (6) used Quantum Monte Carlo methods to obtain the CPs. Olevano et al. (7) calculated CPs by using ab initio Green's function approximation. The DFT methods with different exchange-correlation functional have been used for calculations CP of some targets (8-10). Most of experimental studies is related to crystalline solids. On the other side, there are only a few studies in the literature for gases. CP of He, Ne, Ar, and Kr gases have been measured by experimentally and it was found they have very good agreement with HF calculations (11-14). Sakurai et al. (15) performed synchrotron CP experiments to study CPs for He, Ar, and Xe and compared them to DFT results.

N_2 gas is used in many applications, such as, food technology, in incandescent light bulbs (as an alternative to Ar), fire suppression systems, photolithography, manufacturing of stainless steels, in tires of racecars and aircraft, and etc. Nitrogen isn't a noble gas and it may be different electronic properties at the different conditions. Therefore, we have measured at the CP values of N_2 at different pressures and determined the variation of CP OF N_2 with increasing pressures.

Materials and Methods

1. Theory

Figure 1 shows the scattering process between a photon and a moving electron, In this process, \vec{P}_1 is the momentum of the incident electron, p_z is the component of electron momentum along with z-axis, \vec{P}_2 is the momentum of the

scattering electron,

$\vec{k} = \vec{k}_1 - \vec{k}_2$ is the scattering vector and w_1 and w_2 is the energy of incident and scattered photons, respectively, and j is the scattering angle.

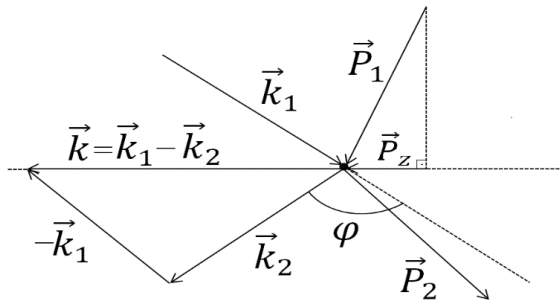


Fig 1. Compton scattering process from an electron with \vec{P}_1 momentum.

The cross-sections for Compton scattering has been calculated for both free electrons and bound electrons [16]. If the IA is valid and the incident energy is small compared to the rest mass energy of electron, m_0c^2 , the Compton cross section is given by

$$\frac{d^2\sigma}{d\Omega dw} = \left(\frac{d\sigma}{d\Omega}\right)_{Th} \frac{w_1}{w_2} \sum \left| \langle f \left| \sum_{l=1}^N e^{i\vec{k}\cdot\vec{r}_l} \right| i \rangle \right|^2 \times \delta(E_f - E_i - w) \quad (1)$$

where \vec{r}_l is the position of the l^{th} atoms and $(d\sigma/d\Omega)_{Th}$ is the nonrelativistic Thomson cross-section and is given by

$$\left(\frac{d\sigma}{d\Omega}\right)_{Th} = \left(\frac{e^2}{mc^2}\right)^2 (\vec{\epsilon}_1 \cdot \vec{\epsilon}_2) \left(\frac{w_2}{w_1}\right)^2 \quad (2)$$

where $\vec{\epsilon}_1$ and $\vec{\epsilon}_2$ are the polarization vectors for incident and scattering photons, respectively (2). For isotropic and spherically averaged systems, Eq. (1) can be rewritten to obtain the following form (12),

$$\frac{d^2\sigma}{d\Omega dw} = \left(\frac{d\sigma}{d\Omega}\right)_{Th} \frac{w_1}{w_2} \frac{m_0}{|\vec{k}|} J(p_z) \approx X(w_2) J(p_z) \quad (3)$$

where

$$J(p_z) = \int \int_{p_x, p_y} n(\vec{p}) dp_x dp_y = \int \int_{p_x, p_y} \chi^*(\vec{p}) \chi(\vec{p}) dp_x dp_y \quad (4)$$

is the CP. $X(w_2)$ is the Ribberfors cross-section. $n(\vec{p})$ is the probability that an electron in the ground state of the system will have momentum \vec{p} . The p_z values is given by

$$q = c \frac{w_2 - w_1 + w_1 w_2 (1 - \cos \varphi) / c^2}{(w_1^2 + w_2^2 - 2w_1 w_2 \cos \varphi)^{1/2}} \quad (5)$$

where c is the velocity of the light (17).

2. Experimental Details

The experimental setup used in this study is shown in Fig 2. All samples sealed in the gas chamber at different pressure were irradiated by photons, which emitted from an annular ^{241}Am radioisotope source with $\sim 1.85 \times 10^{11}$ Bq activity. The scattered photons detected by using a HPGe detector that have a Be window of 12mm, a diameter of 0.16mm, an active area of 200mm² and a resolution ~ 182 eV at 5.9keV. The detector was coupled a Tennelec 244 model amplifier and Ortec 926 model Analogue Digital Converter (ADC). The data were recorded into 4096 channels of Multichannel Analyzer (MCA). The measurements time was 4.0×10^5 s. After removing the gas out of the gas chamber a background measurement was carried out to determine the scattering from the chamber's walls and the gas chamber's window made from hostaphan. The scattering angle was 163° . A typical scattering spectrum from N₂ measured at 5 bars is shown in Figure 3.

To obtain the Compton Profile $J(P_z)$, the raw data $M(w)$ has to be corrected for some effects

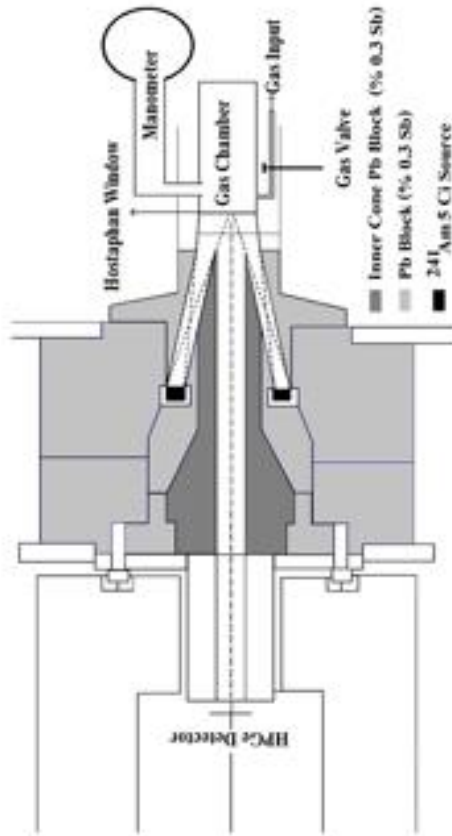


Fig 2. Experimental Setup.

$$C(w) = G(w)X(w)A(w)[M(w) - B(w)] \quad (6)$$

where $B(w)$ is the background, $X(w)$ is the inelastic scattering cross section correction, $A(w)$ is the sample self-absorption correction and $G(w)$ is the efficiency correction of the detector. After all corrections, the new data is deconvoluted with a detector resolution function $R(w)$, and then normalized by using (2).

$$\int_{-\infty}^{+\infty} J(P_z) dz = \frac{1}{T} \int_{-\infty}^{+\infty} (C(w) * R(w)) dw \frac{dq}{dw} = N \quad (7)$$

Area under the Compton Profile equals to the number of electrons per unit cell of the target. T is the normalization constant and $*$ indicates convolution (2).

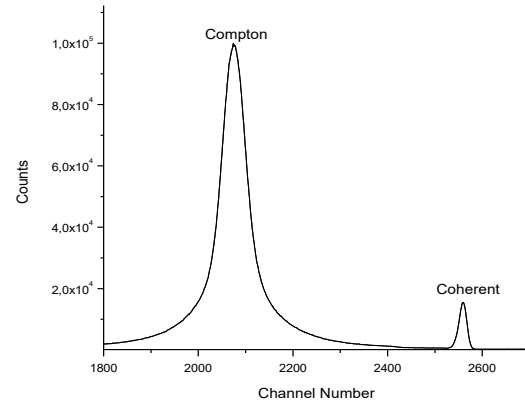


Fig 3. A typical scattering Spectrum for N_2 at the 5 bars pressure.

Results

The measurement time was about five days ($\sim 4.0 \times 10^5$ s) and then a measured background spectrum were subtracted from each spectra to eliminate the environmental effects arisen from spectrometer; i.e. scatterings from hostaphan window and walls of the gas chamber and photons from the radioactive source which never impinge upon the gas chamber. The multiple scattering effects arisen from sample and the walls of gas chamber were corrected during the calculation procedure. Each spectrum was evaluated by a Matlab Code including multiple scattering corrections based on an analytical method explained by Weyrich (17), the self-absorption contribution of gas, deconvolution procedure, and absorption corrections of gas chamber' window, detector window and air between these windows.

In Table 1, we have listed the values of measured Compton Profiles for N_2 gas at different pressures. The previous experimental results measured by Eisenberg and Reed (12), in which a 160 keV ^{123m}Te γ -ray source was used together with a Ge(Li)

detector, also tabulated in Table 1. Besides, the theoretical results calculated by using restricted-Hartree-Slater (RHF) wave functions (18) have been doubled and added the 1s core electrons' contributions, for the purpose of a comparison, have also been presented in Table 1. In addition to these work, there is one important work available in the literature (19). Since these experimental results are a good agreement with the experimental and theoretical values of Eisenberger and Reed (12) they aren't included in Table 1.

Table 1. List of calculated $J(Pz)$ values of N_2 at different Pressure

Pz	$J(Pz)$					Theo(18)	Ref (12)
	Pressure (bars)						
	1.0	2.0	3.0	4.0	5.0		
0	5.070	4.750	4.760	4.740	4.610	5.343	5.271
0.1	4.990	4.680	4.710	4.690	4.580	5.299	5.228
0.2	4.850	4.560	4.640	4.620	4.550	5.169	5.100
0.3	4.650	4.450	4.580	4.530	4.480	4.964	4.896
0.4	4.500	4.320	4.400	4.430	4.320	4.689	4.627
0.5	4.230	4.170	4.120	4.230	4.130	4.364	4.309
0.6	3.950	3.830	3.900	4.090	3.980	4.006	3.959
0.7	3.300	3.500	3.520	3.690	3.500	3.629	3.593
0.8	3.080	3.260	3.390	3.380	3.330	3.251	3.227
0.9	2.690	2.900	3.170	3.080	3.000	2.887	2.874
1	2.500	2.760	2.840	2.740	2.720	2.546	2.545
1.2	1.830	2.270	2.220	2.110	2.130	1.958	1.982
1.4	1.680	1.910	1.930	1.840	1.760	1.503	1.550
1.6	1.190	1.320	1.180	1.340	1.290	1.168	1.230
1.8	0.697	0.898	0.908	1.010	0.970	0.922	0.989
2	0.621	0.679	0.823	0.808	0.798	0.751	0.805
2.5	0.430	0.460	0.566	0.463	0.469	0.504	0.524
3	0.367	0.390	0.439	0.404	0.413	0.378	0.400
3.5	0.232	0.314	0.278	0.275	0.291	0.295	0.299
4	0.209	0.263	0.195	0.215	0.278	0.234	0.238
5	0.099	0.165	0.095	0.124	0.142	0.148	0.147
6	0.099	0.132	0.090	0.108	0.083	0.083	0.086
7	0.012	0.027	0.041	0.101	0.090	0.053	0.048
8	0.018	0.004	0.016	0.039	0.045	0.034	0.030
9	0.016	0.016	0.001	0.007	0.001	0.022	0.019
10	0.013	0.009	0.001	0.008	0.000	0.015	0.009

Discussion

There is a good agreement between our results and theoretical results of Eisenberger (18) and experimental results of Eisenberger and Reed (12) at bigger p_z values ($p_z > 0.5 a.u.$). Our experimental results at 1.0 bar have better agreement with the theoretical and experimental result listed in Table 1. In addition, when $p_z \leq 0.5 a.u.$ the Compton Profile values decrease with increasing pressure up to 5 bars. At $p_z \leq 0.5 a.u.$ values, there are fluctuations in CP values and they may slightly change the resolution of the spectrometer. Nevertheless, these fluctuations don't affect the precision and accuracy of the Spectrometer.

Another important parameter in the Compton Profile calculations is normalizations. In practice, it has to be done over a finite range. Here it helps those outer electrons of an atom, which have more diffuse configurational wavefunctions, possess more localized momentum wavefunctions and thus are concentrated at the peak of the Profile. The wings of the Profile represent the wider momentum distribution of the inner shell electrons, which are conversely more concentrated in the configuration space and very little affected by the effects like chemical bonding. Therefore, sufficiently wide finite limits in the normalization (there from $p_z = 0$ to 10) will yield the same number of electrons the concentration of the outer electrons in the peak is also the reason for sensitivity of Compton Profiles for ionization, chemical bonding etc. After normalization, it was found the normalization values are 6.48. 6.87. 6.89. 6.99. and 6.88 at different pressures from 1 bar to 5 bars, respectively. These values almost equal to $N/2 = 7$. namely these values give us the half of the total electron number of one N_2 molecule.

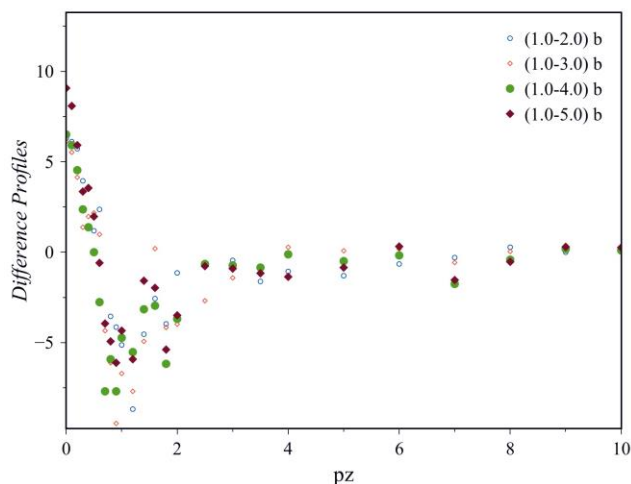


Fig 4. Difference Profiles of N_2 .

In order to investigate the changes of the Compton Profile values, hereafter called the difference profile, between $J(p_z)$ at 1 bar and $J(p_z)$ at other pressures are given by

$$DJ(p_z) = \left[J(p_z) \right]_{1 \text{ bar}} - \left[J(p_z) \right]_{x \text{ bars}} \quad (8)$$

where $x = 2, 3, 4, \text{ and } 5$

Figure 4 illustrates difference profiles for different pressures. Since the difference profiles between the sets of data are fairly small it is necessary to present the data as differences, in order to get sense of proportion into data, the differences are plotted as a percentage of the peak height of CP at 1.0 bar, namely 5.070. At this stage of data analysis procedures it should be noted that no special significance should be attached to CP values listed in Table 1. The only feature of interest is differences between pairs of profiles described by Eq. (8).

When $p_z \in 0.5 \text{ a.u.}$ the difference profiles have important values, especially at the peak of the Profile. Especially, at $p_z = 0$ they change between ~ 6.0 and 9.0% . In this region, the electrons are strongly affected by ionization and chemical bonding. We think

that increasing pressure give rise to more ionization and this lead to a decreasing of Compton Profile values at the peak of rofile and near region. Since the wings of the Profile don't affect from ionization and the profile have some fluctuations there.

As a conclusion, we found that the Compton Profiles changes with increasing pressures. Especially peak of the Profile the changes reach up to 9.0% . Nevertheless, to understand better the changes of Compton Profile with pressure we have to measure the Compton Profile different pressure, more accurate detectors and spectrometer, and intense photon source; such as synchrotron radiation.

References

- [1] Cooper MJ, 1985. Compton-Scattering and Electron Momentum Determination. Reports on Progress in Physics. 48. 415-481.
- [2] Williams BG, 1977. Compton Scattering: The Investigation of Electron Momentum Distributions: McGraw-Hill International.
- [3] Yang F, Hamilton JH, 1996. Modern Atomic and Nuclear Physics: McGraw-Hill Book Co.
- [4] Biggs F, Mendelsohn LB, Mann JB, 1975. Hartree-Fock Compton profiles for the elements. Atomic Data and Nuclear Data Table. 16. 201-309.
- [5] Huotari S, Soininen JA, Pykkanen T, Hamalainen K, Issolah A, Titov A, McMinis J, Kim J, Esler K., Ceperley DM, Holzmann M, Olevano V, 2010. Momentum Distribution and Renormalization Factor in Sodium and the Electron Gas. Physical Review Letters. 105. 086403.
- [6] Holzmann M, Bernu B, Pierleoni C, McMinis J, Ceperley DM, Olevano V, Delle Site L, 2011. Momentum Distribution of the Homogeneous Electron Gas. Physical Review Letters. 107. 110402.

- [7] Olevano V, Titov A, Ladisa M, Hamalainen K, Huotari S, Holzmann M, 2012. Momentum distribution and Compton profile by the ab initio GW approximation. *Physical Review B*. 86. 195123.
- [8] Erba A, Pisani C, Casassa S, Maschio L, Schutz M, Usvyat D, 2010. MP2 versus density-functional theory study of the Compton profiles of crystalline urea. *Physical Review B*. 81. 165108.
- [9] Pisani C, Erba A, Casassa S, Ito M, Sakurai Y, 2011. Anisotropy of the electron momentum distribution in alpha-quartz investigated by Compton scattering and ab initio simulations. *Physical Review B*. 84. 245102.
- [10] Pisani C, Ito M, Sakurai Y, Yamaki R, Ito M, Erba A, Maschio L, 2011. Evidence of instantaneous electron correlation from Compton profiles of crystalline silicon. *Physical Chemistry Chemical Physics*. 13. 933-936.
- [11] Eisenberger P, Platzman PM, 1970. Compton Scattering of X-Rays from Bound Electrons. *Physical Review A*. 2. 415-.
- [12] Eisenberger P, Reed WA, 1972. Gamma-Ray Compton-Scattering - Experimental Compton Profiles for He, N₂, Ar, and Kr. *Physical Review A*. 5. 2085.
- [13] Holm P, Ribberfors R, 1989. 1st Correction to the Nonrelativistic Compton Cross-Section in the Impulse Approximation. *Physical Review A*. 40. 6251-6259.
- [14] Jaiswal P, Shukla A, 2007. Kinetically balanced Gaussian basis-set approach to relativistic Compton profiles of atom. *Physical Review A*. 75. 022504.
- [15] Sakurai H, Ota H, Tsuji N, Ito M, Sakurai Y, 2011. Accurate Compton scattering measurements of noble gases: the importance of electron correlations in heavy atoms. *Journal of Physics B-Atomic Molecular and Optical Physics*. 44. 065001.
- [16] Eisenberger P, Reed WA, 1974. Relationship of Relativistic Compton Cross-Section to Electrons Velocity Distribution. *Physical Review B*. 9. 3237-3241.
- [17] Weyrich W, 1975. Electron Momentum Distribution in Solid Potassium Fluoride. Studied by Compton-Scattering. *Berichte Der Bunsen-Gesellschaft-Physical Chemistry Chemical Physics* 79. 1085-1095.
- [18] Eisenberger P, 1972. Compton-Profile Measurements of N₂, O₂, and Ne Using Silver and Molybdenum X-Rays. *Physical Review A*. 5. 628.
- [19] Paakkari T, Merisalo M, 1975. Experimental Compton Profile of N₂. *Chemical Physics Letters*. 33. 432-435.